

# Increased Expression of Plasminogen Activator Inhibitor-1 in Cardiomyocytes Contributes to Cardiac Fibrosis after Myocardial Infarction

Kyosuke Takeshita,\* Mutsuharu Hayashi,\*  
Shigeo Iino,\* Takahisa Kondo,\* Yasuya Inden,\*  
Mitsunori Iwase,<sup>†</sup> Tetsuhito Kojima,<sup>†</sup>  
Makoto Hirai,<sup>†</sup> Masafumi Ito,<sup>‡</sup> David J. Loskutoff,<sup>§</sup>  
Hidehiko Saito,<sup>¶</sup> Toyoaki Murohara,\* and  
Koji Yamamoto<sup>||</sup>

From the Department of Cardiology,\* Nagoya University Graduate School of Medicine, Nagoya, Japan; the Department of Medical Technology,<sup>†</sup> Nagoya University School of Health Sciences, Nagoya, Japan; the Departments of Pathology<sup>‡</sup> and Transfusion Medicine,<sup>||</sup> Nagoya University Hospital, Nagoya, Japan; Nagoya National Hospital,<sup>¶</sup> Nagoya, Japan; and the Department of Cell Biology,<sup>§</sup> Division of Vascular Biology, The Scripps Research Institute, La Jolla, California

**Plasminogen activator inhibitor-1 (PAI-1) plays a critical role in tissue fibrosis by inactivating matrix metalloproteinases, which might effect on the progression of left ventricular dysfunction. However, little has been known about the expression of PAI-1 during cardiac remodeling. We used a mouse model of myocardial infarction (MI) by coronary ligation, in which the progression of left ventricular remodeling was confirmed by echocardiography. Histological examination showed that interstitial and perivascular fibrosis progressed in the post-MI (PMI) heart at 4 weeks after the procedure. We observed the dramatic induction of cardiac PAI-1 mRNA and PAI-1 antigen in plasma in the PMI mice, as compared with the sham-operated (sham) mice. *In situ* hybridization analysis demonstrated that strong signals for PAI-1 mRNA were localized to cardiomyocytes in the boarder of infarct area and around fibrous lesions, and to perivascular mononuclear cells, which seemed to be mast cells, only in hearts of the PMI mice. Importantly, less development of cardiac fibrosis after MI was observed in mice deficient in PAI-1 as compared to wild-type mice. The mRNA expression of cytokines, transforming growth factor- $\beta$ , and tumor necrosis factor- $\alpha$ , was also increased in hearts of the PMI mice, but not in the sham mice. These observations suggest that cardiomyocytes and mast cells contribute to the increased PAI-1 expression, resulting in the development of interstitial and perivascular fibrosis in the PMI heart, and that the regional induction of**

**cytokines may be involved in this process. (*Am J Pathol* 2004, 164:449–456)**

Myocardial infarction (MI) is frequently accompanied by fibrous changes and by left ventricular (LV) remodeling, which may result in the heart failure. Cardiac fibrosis, which is demonstrated by accumulation of extracellular matrix (ECM), causes diastolic dysfunction,<sup>1</sup> and may provide the structural substrate for arrhythmogenicity, thus contributing to the progression of heart failure and sudden death.<sup>2</sup> The progression of LV remodeling during the repair process after MI is mostly determined by the degradation of myocardial ECM.<sup>3–5</sup> In this context, the accumulation or degradation of cardiac ECM in MI patients is one of the most important issues to improve the prognosis. The principal system, which could regulate ECM metabolism in hearts, is the matrix metalloproteinases (MMPs)-tissue inhibitor of metalloproteinases (TIMPs) pathway.<sup>6</sup> Indeed, the inappropriate elevation of MMP's activity impairs LV remodeling and leads to the pump failure in the infarct heart.<sup>5</sup>

Plasmin, one of the serine proteases, is an active enzyme of the fibrinolytic system, and has a proteolytic activity as well. It plays a critical role in the degradation of ECM directly and by activation of pro-MMPs in cardiac tissues.<sup>6</sup> The fibrinolytic potential in the tissue is determined by balance between urokinase-type plasminogen activator (u-PA) and plasminogen activator inhibitor (PAI)-1. A significant role of u-PA and MMPs has been demonstrated in cardiac rupture and scar formation after MI.<sup>7,8</sup> u-PA and MMPs could degrade ECM in the scar of infarct area, thus contributing to the vulnerability of cardiac wall. The activity of u-PA and MMPs is primarily controlled by their endogenous inhibitors, PAI-1 and TIMPs. PAI-1, which was shown to be expressed in mammalian cardiomyocytes,<sup>7</sup> is implicated in the process of the cardiac remodeling by inhibiting activation of MMPs as well as plasmin generation. PAI-1 could inhibit inter-

Supported by grants-in-aid from the Ministry of Education, Science, Sports, and Culture; the Ministry of Health and Welfare; and by funds from Comprehensive Research on Aging and Health, Japan.

Accepted for publication October 13, 2003.

Address reprint requests to Dr. K. Yamamoto, Dept. of Transfusion Medicine, Nagoya University Hospital, 65 Tsurumai, Showa, Nagoya 466-8560, Japan. E-mail: kojij@med.nagoya-u.ac.jp.

stitial proteolysis, especially in the infarct heart during the chronic phase, which determines the prognosis of MI patients. We have focused on the pathological role of PAI-1 in the cardiac repair, and thus, investigated the expression and localization of PAI-1 in the heart of an *in vivo* model of MI.

In this report, we observed the dramatic induction of PAI-1 in a mouse model of infarct heart in the chronic phase. More specifically, cardiomyocytes and mast cells in the boarder of infarct area and around fibrous lesions, expressed abundant PAI-1 mRNA in the post-MI (PMI) mice. Experiments using mice deficient in PAI-1 suggests that increased expression of cardiac PAI-1 may contribute to the development of fibrous change after MI. Furthermore, we observed increases in the regional expression of inflammatory cytokines, tumor necrosis factor (TNF)- $\alpha$ , and transforming growth factor (TGF)- $\beta$ , both of which dramatically induce PAI-1 expression *in vivo*.<sup>9,10</sup> Thus, the response of cardiomyocytes and mast cells in the induction of PAI-1 in the infarct heart could be relevant to the progression of cardiac fibrosis, and the regional induction of inflammatory cytokines may be involved in this process.

## Materials and Methods

### *A Mouse Model of Myocardial Infarction and LV Remodeling*

All procedures were performed according to the protocol approved by the Animal Care and Use Committee of Nagoya University. MI was developed in male 6-week-old C57BL/6J mice ( $n = 15$ ) by ligating the left coronary artery.<sup>11</sup> We provided the sham-operated animals, which underwent the same procedure without ligation of the artery, to exclude the influence of the surgical procedure itself to the experimental results. All of the MI mice had infarct area more than 40% of the LV and showed impairment of systolic function. We examined the progression of LV remodeling with echocardiograms at the point of 2 and 4 weeks after surgical procedure. Echocardiographic studies were performed under anesthesia with ketamine (0.065 mg/body weight g) and xylazine (0.013 mg/body weight g). Imaging was obtained with an Acuson (Mountain View, CA) Sequoia model 256 clinical echocardiograph fitted with an 8-MHz sector-scanning probe.<sup>12</sup> All of the MI mice demonstrated lower than 50% of fractional shortening (%FS) and enlarged diastolic LV diameter (dLVD) more than 3.5 mm at 2 weeks after the procedure. We performed the same experiment using mice deficient in PAI-1<sup>13</sup> as wild-type mice.

### *Plasma and Tissue Preparation*

After echocardiographic studies at 4 weeks after surgical procedure, mice were sacrificed by overdose inhalation anesthesia with ether and cervical dislocation. The plasma was collected, and then several tissues (eg, heart, liver, lung, kidney, adrenal, and adipose tissues) were rapidly excised by standard dissection technique,

and either minced, quickly frozen in liquid nitrogen for preparation of total RNA, or fixed in chilled 4% paraformaldehyde and embedded in paraffin for histological examination, *in situ* hybridization, and immunohistochemistry.

### *PAI-1 Enzyme-Linked Immunosorbent Assay*

PAI-1 antigen levels in plasma were quantified by a sandwich enzyme-linked immunosorbent assay as described<sup>14</sup> with minor modification. Briefly, polystyrene microtiter plates were coated with 50  $\mu$ l of a rabbit polyclonal anti-mouse PAI-1 IgG prepared by naked DNA immunization method described previously,<sup>15</sup> at a concentration of 20  $\mu$ g/ml in 50 mmol/L of bicarbonate buffer (pH 9.5) with 0.02% NaN<sub>3</sub> (0.2 g). After allowing the plate to remain at 4°C overnight, the plate was washed four times with washing buffer [phosphate-buffered saline (PBS) with 0.05% Tween 20], blocked with 150  $\mu$ l/well of blocking buffer (PBS with 1% bovine serum albumin), and then washed four times with washing buffer. Samples (or positive control, consisting of GST-mouse PAI-1) were added (50  $\mu$ l/well), incubated at room temperature for 5 hours, and then washed four times with washing buffer. Plates were further prepared by adding 50  $\mu$ l/well of rabbit anti-mouse PAI-1 IgG (5  $\mu$ g/ml) which was biotinylated using the ECL protein biotinylation module (Amersham Biosciences, Tokyo, Japan). After washing four times with washing buffer, ExtrAvidin peroxidase (diluted 1:1000 in an assay buffer consisting of PBS, pH 7.4, bovine serum albumin, 1%, and Tween 20, 0.05%; Sigma, St. Louis, MO) was added to each well (100  $\mu$ l/well). Plates were then developed using 100  $\mu$ l/well of freshly prepared developing solution for horseradish peroxidase, o-phenylenediamine (0.75 g/L), and H<sub>2</sub>O<sub>2</sub> were added. Plates were further incubated to allow color development, followed by termination of the reaction with 4 N H<sub>2</sub>SO<sub>4</sub> (50  $\mu$ l/well). Absorbance was read at 490 nm, and the detection limit in this assay was 200 pg/ml (41.7 pmol/L). Experiments were performed in duplicate and the results were presented as the mean  $\pm$  SD.

### *RNA Extraction and Quantitative Reverse Transcriptase-Polymerase Chain Reaction (RT-PCR)*

Total tissue RNA was isolated using STAT-60 total RNA isolation reagent (Stratagene, La Jolla, CA). One  $\mu$ g of each tissue RNA was reverse-transcribed, and then, the concentration of PAI-1, TGF- $\beta$ , TNF- $\alpha$ , and  $\beta$ -actin mRNAs in the tissues was determined by real-time quantitative RT-PCR with ABI Prisms 7700 Sequence Detection (Perkin-Elmer Biosystems, Foster City, CA) and SYBR Green PCR Kit (Perkin-Elmer Biosystems), according to the manufacturer's recommendations. A synthetic DNA template containing the sequences for the upstream and downstream primers for PAI-1, TGF- $\beta$ , TNF- $\alpha$ , and  $\beta$ -actin (internal control) was used as a standard. The sequences of primer pairs used to quantify mRNAs of the above

genes were described previously.<sup>16,17</sup> Various concentrations of the standard DNA template (eg,  $1 \times 10^4$  to  $10^9$  molecules/ $\mu$ l) were used for the calibration curve for each primer set. After 35 cycles of PCR reaction (94°C for 30 seconds, 60°C for 30 seconds, and 72°C for 30 seconds), the amount of gene transcripts was calibrated by the comparison with the standard curve. All of RT-PCR experiments were performed in duplicate. The PCR products were electrophoresed on a 2% agarose gel and visualized with ethidium bromide to confirm the proper PCR amplification (data not shown).

### In Situ Hybridization

*In situ* hybridization was performed using <sup>35</sup>S-labeled anti-sense riboprobes, as described previously.<sup>16,17</sup> After hybridization, the slides were dehydrated by immersion in a graded alcohol series containing 0.3 mol/L NH<sub>4</sub>Ac, and dried. Then, the slides were coated with NTB2 emulsion (1:2 in water; Eastman Kodak, Rochester, NY), and exposed in the dark at 4°C for 4 to 10 weeks. The slides were developed for 2 minutes in D19 developer (Kodak), fixed, washed in water, and counterstained with hematoxylin and eosin (H&E). No specific hybridization signal could be detected in parallel sections using <sup>35</sup>S-labeled sense probes in each experiment (data not shown).

### Immunohistochemistry

Immunohistochemical staining was performed using the Histostain-SP kit (Zymed Laboratories, South San Francisco, CA) according to the manufacturer's recommendations. Briefly, the tissue sections were deparaffinized, treated with 2% hydrogen peroxide, and incubated with 10% normal goat serum for 30 minutes. The slides were then incubated with 10  $\mu$ g/ml of rabbit anti-human PAI-1 antibody that cross-reacts to mouse PAI-1 (a kind gift of Dr. Y. Eguchi, Shiga University of Medical Science, Shiga, Japan), containing 0.1% goat serum at 4°C overnight, followed by incubation for 1 hour at 25°C. In control experiments, tissues were incubated with normal rabbit IgG instead of the primary antibody. The slides were then washed and treated sequentially with biotinylated goat anti-rabbit IgG diluted in 1:100 (Zymed Laboratories), streptavidin-peroxidase conjugate, and aminoethylcarbazole chromogen containing 0.03% hydrogen peroxide. The slides were counterstained with hematoxylin and mounted in GVA-mount (Zymed Laboratories).

### Histopathological Analysis

Histopathological and morphometric analysis of cardiac tissues was performed by a single investigator who was unaware of the treatment protocol. The tissue sections ( $n = 10$ ) were stained with H&E for overall morphological analysis, with May-Giemsa staining or toluidine blue method to detect degranulating mast cells,<sup>18</sup> or with Sirius Red F3BA (0.1% solution in saturated aqueous picric acid) to demonstrate collagen matrix indicating

fibrous changes.<sup>19</sup> The progression of perivascular fibrosis was evaluated by comparing the perivascular area to the total vessel area, as described previously.<sup>20</sup> We analyzed the short-axis images of 6 to 10 coronary arteries per cardiac tissue section. The inner border of the lumen and outer border of the tunica media were traced in each image, and then, calculated by use of Win ROOF version 5.02 (MITANI Corp., Fukui, Japan). The area of fibrosis surrounding the coronary arteries was measured and the ratio of perivascular fibrosis was determined by dividing fibrous areas by vessel areas.

### Statistical Analysis

All data are presented as the mean  $\pm$  SD. The paired data were compared by paired Student's *t*-test. Comparisons between the sham and PMI groups were tested by the unpaired Student's *t*-test. Multiple comparisons among four groups were performed by one-way analysis of variance followed by Fisher's protected least significant difference tests. A *P* value <0.05 was considered significant.

## Results

### LV Function of the PMI Mouse

We evaluated LV function of the PMI mice and sham mice with M-mode echocardiogram (Figure 1A). The image of a sham mouse shows normal thickness and contraction of the LV wall. In the image of a PMI mouse, a dilated LV chamber with thinning of the anterior wall was demonstrated. Reduced wall motion of the viable myocardium was also observed in the posterior wall of a PMI mouse. The quantitative echocardiographic data on the LV function at 4 weeks after procedure are shown in Figure 1, B and C. The average %FS was significantly lower in the PMI group ( $46.8 \pm 5.8\%$ ) as compared with the sham group ( $75.6 \pm 1.8\%$ ) ( $n = 15$ , respectively;  $P < 0.05$ ; Figure 1B). The evaluation of the LV end-diastole revealed that the PMI group had larger diameter ( $3.75 \pm 0.28$  mm) than the sham group ( $2.38 \pm 0.14$  mm) ( $n = 15$ , respectively;  $P < 0.05$ ; Figure 1C). The LV function between 2- and 4-week intervals after the procedure was not significantly different between two groups (data not shown).

### PAI-1 Expression in the PMI Mouse

We analyzed the expression of systemic and regional PAI-1 expression in cardiac tissues of the PMI and sham mice at 4 weeks after surgical procedure. Total PAI-1 antigen level in plasma was elevated in the PMI mice, but not in the sham mice ( $4.28 \pm 1.4$  ng/ml versus  $0.29 \pm 0.76$  ng/ml;  $n = 7$ , respectively;  $P < 0.05$ ; Figure 2A). The expression of PAI-1 mRNA dramatically increased (13-fold) in the cardiac tissue of noninfarct areas in the PMI mice, as compared with the sham mice ( $n = 7$ , respectively;  $P < 0.01$ ; Figure 2B). However, no significant induction of PAI-1 mRNA was detected in other organs (eg,

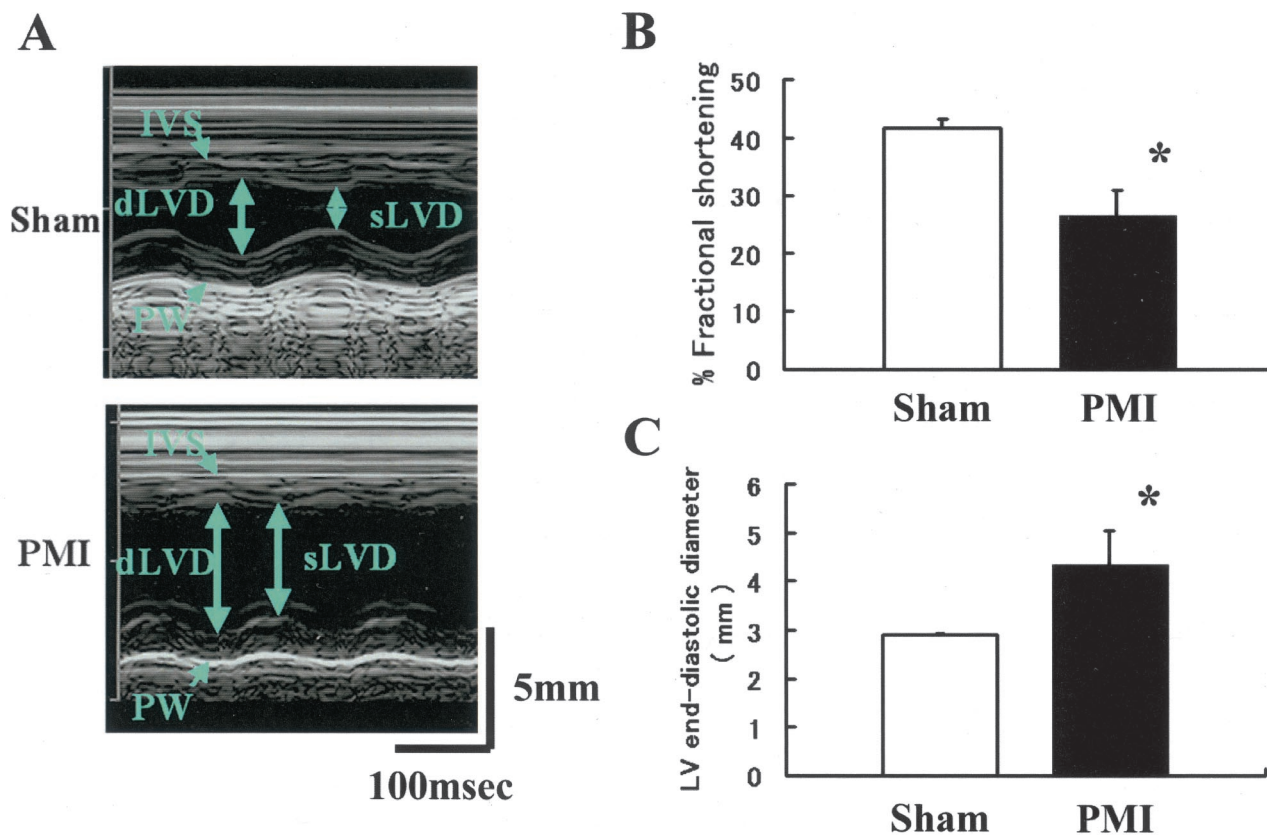


**Figure 1.** LV function of the PMI mouse. **A:** M-mode echocardiograms. We performed M-mode echocardiograms of the sham (top) and PMI (bottom) mice 4 weeks after coronary ligation. The images from sham mice showed normal contraction and wall thickness (IVS, intraventricular septum; PW, posterior wall; dLVD, diastolic left ventricular dimension; sLVD, systolic left ventricular dimension). The image of the PMI mice showed thinned IVS, dilated dLVD, and reduced wall motion in the PW. **B:** Percentage of fractional shortening (%FS) of the sham and PMI mice. **C:** Endodiastolic diameter of LV of the sham and PMI mice. The data are presented as the mean  $\pm$  SD ( $n = 15$ , respectively). \*,  $P < 0.05$ .

lung, kidney, adipose, liver, adrenal) of the PMI mice (data not shown). These results suggest that increased expression of cardiac PAI-1 contributes to the elevation of systemic plasma level of PAI-1 in the PMI mice. The results obtained by *in situ* hybridization analysis on the cardiac tissue (Figure 3) were consistent with the RT-PCR data. Although no signals for PAI-1 mRNA were detected in hearts of the sham mice (Figure 3A), strong signals for PAI-1 mRNA were localized to cardiomyocytes of the PMI hearts (Figure 3B), especially in the marginal zone of fibrous changes (Figure 3C). Cardiomyocytes and fibroblasts in this region specifically expressed abundant

PAI-1 mRNA (Figure 3C). High expression of PAI-1 mRNA was also observed in smooth muscle cells and perivascular cells surrounding arteries (Figure 3D), which seemed to be mast cells. Although no mast cell invasion to perivascular and interstitial regions was observed in the sham mice as previously reported,<sup>21</sup> we occasionally detected degranulating mast cells in perivascular area with the development of fibrosis in the PMI mice (Figure 3E). We counted the number of mast cells per field of view (magnification,  $\times 400$ ) both in the PMI and sham mice ( $n = 10$ ) and observed two to three mast cells in perivascular area only in the PMI mice (data not shown). We could find no PAI-1 signals in vascular endothelial cells in both groups. Immunohistochemical analysis showed the positive staining for PAI-1 antigen in cells distributed in interstitial fibrous region (Figure 3F), which was consistent with *in situ* hybridization analysis.

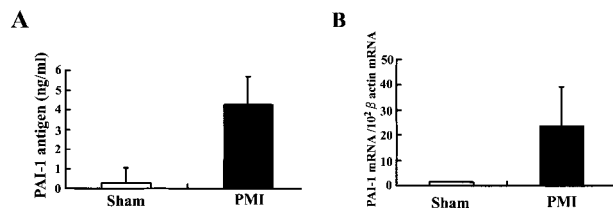


**Figure 2.** PAI-1 expression in the PMI mouse. The plasma and cardiac tissues were collected at 4 weeks after surgical procedure, and then, PAI-1 antigen in plasma and cardiac expression of PAI-1 mRNA were quantitated as described in Materials and Methods. **A:** Total PAI-1 antigen in plasma of the sham and PMI mice. **B:** The expression levels of PAI-1 mRNA in hearts of the sham and PMI mice. The results were standardized by the expression levels of  $\beta$ -actin mRNA. The data are presented as the mean  $\pm$  SD ( $n = 7$ , respectively).

#### Coronary Perivascular and Endocardial Fibrosis after MI in Wild-Type and PAI-1-Deficient Mice

We induced MI in PAI-1-deficient mice<sup>13</sup> by the same procedure, as described in the Materials and Methods. Recently, it was reported that PAI-1-deficient mice often died of cardiac rupture within 7 days after coronary ligation.<sup>22</sup> As social stress and hyperactivity would deteriorate

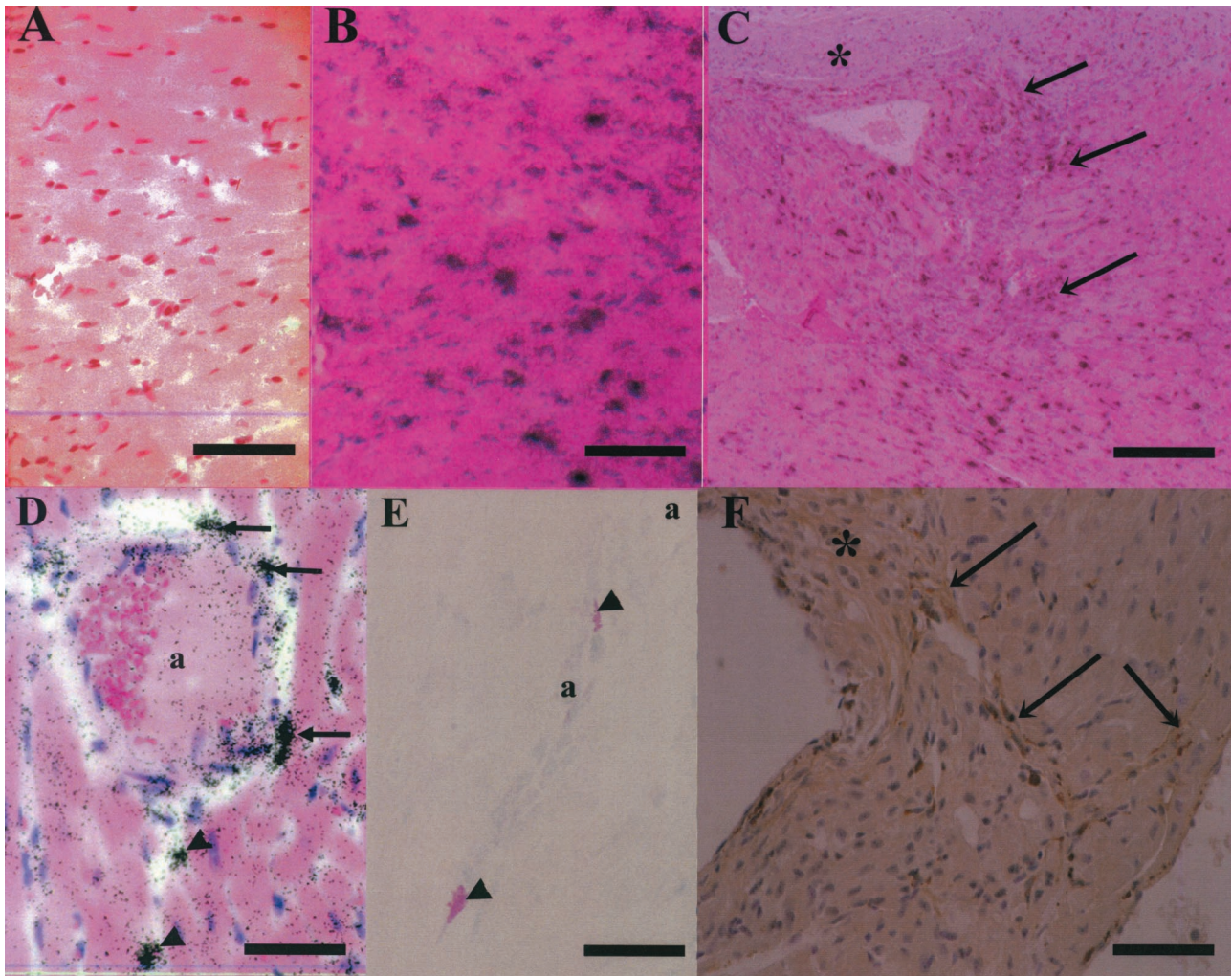


**Figure 3.** *In situ* hybridization and immunohistochemistry for PAI-1 in hearts of the sham and PMI mice. *In situ* hybridization analysis for PAI-1 mRNA in hearts of the sham and PMI mice using <sup>35</sup>S-labeled anti-sense riboprobes (**A–D**). **Black dots** denote signals for PAI-1 mRNA. **A:** Myocardium of the sham mouse. **B:** Myocardium in noninfarct areas of the PMI mouse. **C:** Interstitial fibrous areas around infarct area in the PMI heart. The **asterisk** denotes infarct area. **Arrows** indicate positive signals for PAI-1 mRNA in cardiomyocytes and/or fibroblasts in the marginal zone of fibrous changes. **D:** Strong signals for PAI-1 mRNA in smooth muscle cells (**arrows**) and likely mast cells (**arrowheads**) around the coronary artery (a) of the PMI heart. **E:** Mast cells around coronary arteries (a) that are positively stained with May-Giemsa. **Arrowheads** denote the degranulating mast cells. **F:** Immunohistochemical staining for PAI-1 antigen in the region of interstitial fibrosis. The **asterisk** denotes infarct area. **Arrows** denote positive staining for PAI-1 in cardiomyocytes and/or fibroblasts. Scale bars: 150  $\mu$ m (**A, B**); 300  $\mu$ m (**C**); 100  $\mu$ m (**D, E**); 600  $\mu$ m (**F**).

rate the mortality in the mouse model of MI,<sup>8</sup> we put mice one by one in a separate cage to remove social stress. Eighty percent of PAI-1-deficient mice maintained in one cage, where four to five mice lived together, suddenly died within a week after the procedure ( $n = 15$ ), whereas only 30% of them died when maintained in a separate cage ( $n = 13$ ). The size of infarct area in PAI-1-deficient mice was almost same with that observed in wild-type mice (data not shown).

Histopathological examination was performed to analyze the progression of cardiac fibrosis at 4 weeks after MI in noninfarct areas of wild-type and PAI-1-deficient mice in comparison with the sham mice. We observed larger fibrous tissues in the endocardial interstitium (Figure 4A) and in perivascular area (Figure 4B) of wild-type mice after MI. However, less progression of cardiac fibrosis as described above, was revealed in PAI-1-deficient mice after MI (Figure 4B). Quantitative evaluation of

perivascular fibrosis was performed in the sham and PMI groups using wild-type and PAI-1-deficient mice, as described in the Materials and Methods (Figure 4C). The PMI groups of wild-type mice showed the significant development of coronary perivascular fibrosis in comparison with the sham groups and with the PMI groups of PAI-1-deficient mice.

#### *Cardiac Expression of Cytokines in the PMI Mouse*

We then investigated the expression of cytokines, TGF- $\beta$  and TNF- $\alpha$ , both of which were shown to be inducers of PAI-1 expression *in vitro*<sup>9</sup> and *in vivo*,<sup>10</sup> in cardiac tissues of the wild-type and PAI-1-deficient mice at 4 weeks after MI (Figure 5). TGF- $\beta$  mRNA expression in hearts of the wild-type mice significantly increased after MI (eg, two-

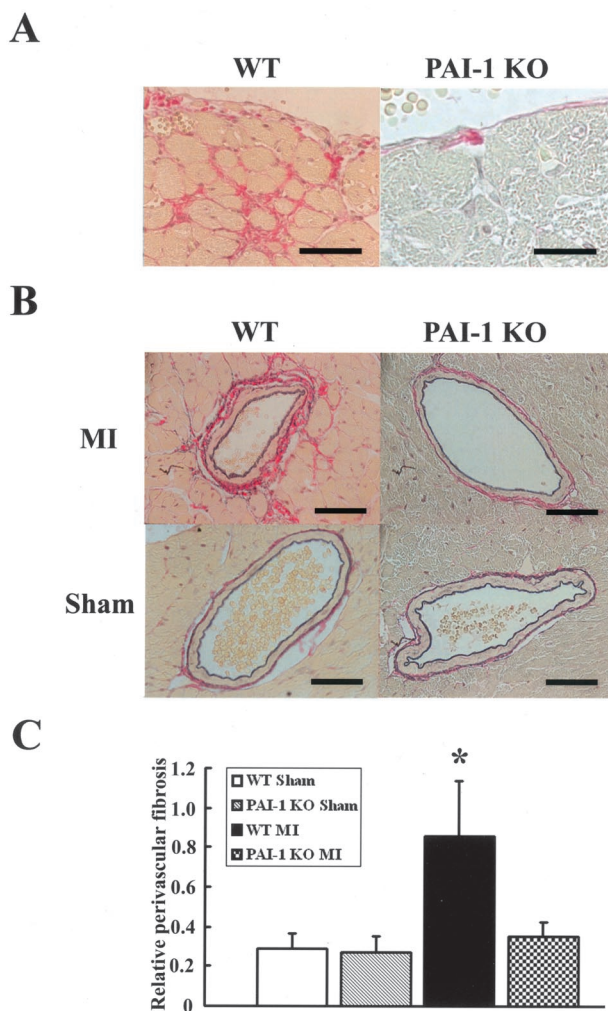


**Figure 4.** Cardiac perivascular fibrosis in PAI-1-deficient mice and wild-type mice after MI. Histopathological examination was performed to analyze the progression of cardiac fibrosis at 4 weeks after MI in noninfarct areas of wild-type and PAI-1-deficient mice in comparison with the sham mice. **A:** Microscopic analysis of endocardium from the sham and PMI hearts of wild-type mice. Cardiac tissue sections were stained with Sirius Red F3BA and the red staining denotes fibrous tissue. **B:** Microscopic analysis of coronary artery sections from the sham and PMI hearts of wild-type or PAI-1-deficient mice by staining with Sirius Red F3BA. Perivascular red portions correspond to fibrous changes. **C:** Quantitative evaluation of perivascular fibrosis was performed in the sham and PMI groups using wild-type (WT) and PAI-1-deficient (PAI-1 KO) mice. The short-axis images of the 6 to 10 coronary arteries per heart section were studied. The data are presented as the mean  $\pm$  SD ( $n = 10$  per group). \*,  $P < 0.05$  versus other groups. Scale bars, 40  $\mu$ m. Original magnifications:  $\times 750$  (A);  $\times 600$  (B).

fold compared to the sham,  $n = 7$ ,  $P < 0.05$ ; Figure 5A, left). Similarly, cardiac expression of TGF- $\beta$  mRNA in PAI-1-deficient mice was also elevated after infarction ( $n = 7$ ,  $P < 0.05$ ; Figure 5A, right). TNF- $\alpha$  mRNA expression in hearts of the wild-type and PAI-1-deficient mice slightly increased after MI in comparison with the sham mice ( $n = 7$ , respectively,  $P = 0.07$ ; Figure 5B).

### Discussion

PAI-1 is a principal inhibitor of plasminogen activators (PAs), which generate plasmin and activate MMPs.<sup>6</sup> The

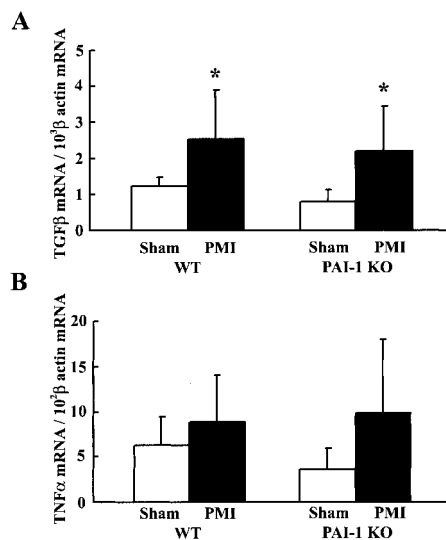


**Figure 5.** Cardiac expression of TGF- $\beta$  and TNF- $\alpha$  mRNA. Quantitative RT-PCR assay was performed to measure mRNA expression of TGF- $\beta$  and TNF- $\alpha$  in noninfarct area of cardiac tissues obtained from the wild-type and PAI-1-deficient mice at 4 weeks after MI in comparison with the sham mice. **A:** TGF- $\beta$  mRNA levels. **B:** TNF- $\alpha$  mRNA levels. The data are presented as the mean  $\pm$  SD ( $n = 7$ , respectively). \*,  $P < 0.05$  versus sham.

regulation of the PA/plasmin system could modulate the accumulation or degeneration of ECM components in the heart as well as in other organs (eg, lung,<sup>23</sup> kidney<sup>24</sup>). Heymans and colleagues<sup>8</sup> reported that adenoviral PAI-1 overexpression resulted in the prevention from cardiac rupture after MI by inhibiting local proteolysis. Thus, PAI-1 regulates the PA/plasmin system, which has been implicated as an important modulator during the process of cardiac repair after MI. Regional PAI-1 induction observed in several pathologies could contribute to the progression of tissue fibrosis.<sup>7,25</sup> In terms of cardiac histopathology, it was reported that perivascular fibrosis in coronary arteries was developed in parallel with increases in PAI-1 expression in genetically obese mice.<sup>26</sup> Moreover, PAI-1-deficient mice were resistant to the progression of coronary perivascular fibrous change in a model of long-term nitric oxide synthase inhibition induced by L-NAME.<sup>20</sup> We also observed that less development of cardiac fibrosis after MI in mice deficient in PAI-1 than wild-type mice (Figure 4), suggesting that PAI-1 deficiency may prevent the increase of collagen deposition by accelerating matrix degradation. Askari and colleagues<sup>22</sup> demonstrated that PAI-1 and myeloperoxidase might play a critical role in cardiac ventricular remodeling after infarction. They revealed that decreased leukocyte infiltration as well as decreased oxidative inactivation of PAI-1 in cardiac infarct area of myeloperoxidase null mice, in which LV remodeling significantly progressed. Taken together, the increased expression of cardiac PAI-1 could contribute to the progression of cardiac fibrosis in the repair process after MI. The timely augmentation of PAI-1 expression in the hearts of MI patients could improve their prognosis because PAI-1 deficiency increased the cardiac rupture in the acute phase of MI.<sup>8</sup>

Recently, it was reported that human cardiomyocytes could produce a large amount of PAI-1 in response to inflammatory cytokines *in vitro*.<sup>27</sup> *In vivo* studies also showed that PAI-1 expression was induced in hearts under such pathological conditions as ventricular hypertrophy<sup>28</sup> and endotoxin-induced sepsis.<sup>16</sup> We previously reported that strong signals for PAI-1 mRNA were localized to cardiomyocytes in a mouse model of premature aging.<sup>29</sup> In the present study, we have demonstrated that coronary ligation in mice resulted in marked hemodynamic alteration (Figure 1) similar to that observed in patients with MI. Importantly, cardiac expression of PAI-1 markedly increased during tissue remodeling (Figure 2), and cardiomyocytes in the border of infarct area produced abundant PAI-1 in our MI model (Figure 3). The expression of inflammatory mediators (eg, inflammatory cytokines,<sup>30</sup> free radicals<sup>11</sup>) would be induced not only in the ischemic area but also in noninfarct area. Indeed, we observed the induction of TGF- $\beta$  and TNF- $\alpha$  mRNA in noninfarct area in the PMI mice, which would induce PAI-1 in cardiomyocytes and fibroblasts. This implies that the elevation of PAI-1 antigen in plasma might reflect the extent of inflammatory response of the cardiac tissue to ischemia. There have been many reports describing the increase of PAI-1 antigen in plasma of MI patients,<sup>31,32</sup> but the mechanism remained to be unclear. Our results suggest that the infarct heart itself would contribute to the prothrombotic state by producing PAI-1, which might cause the resistance to fibrinolytic therapy by t-PA.<sup>33</sup> Meantime, the infiltration of mast cells was observed only in hearts of the PMI mice. It was found that mast cells could induce the proliferation of fibroblasts<sup>34</sup> and be relevant to fibrous diseases.<sup>35</sup> Especially, perivascular mast cells, which have been implicated in cardiovascular diseases<sup>36</sup> and increased in failing hearts,<sup>37,38</sup> could produce significant levels of PAI-1 (Figure 3). These observations strongly suggest that cardiac mast cells have a large potential to produce PAI-1 during pathological processes such as inflammatory response.<sup>39</sup>

Besides degrading ECM components and activating MMPs, the PA/plasmin system may be involved in the activation of growth factors in the ECM.<sup>40</sup> For example, plasmin converts latent TGF- $\beta$  to active TGF- $\beta$ , which could mediate collagen deposition, and this TGF- $\beta$  activation was reduced in u-PA-deficient mice.<sup>41</sup> These findings indicate that the u-PA/plasmin system could activate TGF- $\beta$  in the repair process after infarction. The present study revealed that TGF- $\beta$  expression in cardiac tissues was similarly elevated in the wild-type and PAI-1-deficient mice after MI (Figure 5), suggesting that not TGF- $\beta$ , but PAI-1 induction is necessary for the progression of cardiac fibrosis (Figure 4). TGF- $\beta$ , produced by smooth muscle cells and inflammatory cells, is also a strong inducer of PAI-1 *in vitro* and *in vivo*.<sup>42,43</sup> and accelerates fibrous changes.<sup>43,44</sup> These findings suggest that increased TGF- $\beta$  in inflammatory lesions stimulates PAI-1 synthesis in cardiomyocytes during cardiac remodeling after MI. Perivascular mast cells, the increased number of which was observed in the PMI mice, is also an important source of cytokines such as TGF- $\beta$ .<sup>45</sup> Thus, a local network of cardiac cells, infiltrating inflammatory cells, and

mast cells in the lesion, might contribute to tissue remodeling and the progression of cardiac fibrosis after MI.

In conclusion, we demonstrated a dramatic induction of PAI-1 that was derived from cardiomyocytes and mast cells in hearts of the PMI mice. PAI-1-deficient mice were resistant to the development of fibrous change after MI, suggesting that increased expression of cardiac PAI-1 may contribute to tissue remodeling and cardiac fibrosis. The regional induction of inflammatory cytokines, such as TGF- $\beta$  and TNF- $\alpha$ , may be involved in this process by stimulating PAI-1 synthesis in cardiac cells.

### Acknowledgments

We thank T. Thinner, T. Yamada, T. Nezu, and K. Sakakura for their expert technical assistance; and Dr. T. Watanabe (Takeda Chemical Industries, Ltd.), Dr. S. Murata (Tanabe Pharmaceutical Co.), and Dr. H. Tsutsui (Kyushu University) for their helpful advice.

### References

- Whittaker P, Boughner DR, Kloner RA: Role of collagen in acute myocardial infarct expansion. *Circulation* 1991, 84:2123-2134
- Zannad F, Dousset B, Alla F: Treatment of congestive heart failure: interfering the aldosterone-cardiac extracellular matrix relationship. *Hypertension* 2001, 38:1227-1232
- Kim HE, Dalal SS, Young E, Legato MJ, Weisfeldt ML, D'Armiento J: Disruption of the myocardial extracellular matrix leads to cardiac dysfunction. *J Clin Invest* 2000, 106:857-866
- Rohde LE, Ducharme A, Arroyo LH, Aikawa M, Sukhova GH, Lopez-Anaya A, McClure KF, Mitchell PG, Libby P, Lee RT: Matrix metalloproteinase inhibition attenuates early left ventricular enlargement after experimental myocardial infarction in mice. *Circulation* 1999, 99:3063-3070
- Li YY, Feldman AM, Sun Y, McTiernan CF: Differential expression of tissue inhibitors of metalloproteinases in the failing human heart. *Circulation* 1998, 98:1728-1734
- Creemers EEJM, Cleutjens J, Smits JFM, Daemen MJAP: Matrix metalloproteinase inhibition after myocardial infarction. A new approach to prevent heart failure? *Circ Res* 2001, 89:201-210
- Creemers EEJM, Cleutjens J, Smits J, Heymans S, Moons L, Collen D, Daemen M, Carmeliet P: Disruption of the plasminogen gene in mice abolishes wound healing after myocardial infarction. *Am J Pathol* 2000, 156:1865-1873
- Heymans S, Luttun A, Nuyens D, Theilmeier G, Creemers E, Moons L, Dyspersin GD, Cleutjens JPM, Shipley M, Angellilo A, Levi M, Nube O, Baker A, Keshet E, Lupu F, Herbert JM, Smits JF, Shapiro SD, Baes M, Borgers M, Collen D, Daemen MJ, Carmeliet P: Inhibition of plasminogen activators or matrix metalloproteinases prevent cardiac rupture but impairs therapeutic angiogenesis and causes cardiac failure. *Nat Med* 1999, 10:1135-1142
- Quax PHA, van den Hoogen CM, Verheijen JH, Padro T, Zeheb R, Gelehrter TD, van Berkel TJC, Kuiper J, Emeis JJ: Endotoxin induction of plasminogen activator and plasminogen activator inhibitor type 1 mRNA in rat tissues *in vivo*. *J Biol Chem* 1990, 265:15560-15563
- Sawdey MS, Loskutoff DJ: Regulation of murine type 1 plasminogen activator inhibitor gene expression *in vivo*: tissue specificity and induction by lipopolysaccharide, tumor necrosis factor- $\alpha$ , and transforming growth factor- $\beta$ . *J Clin Invest* 1991, 88:1346-1353
- Hayashidani S, Tsutsui H, Shiomi T, Suematsu N, Kinugawa S, Ide T, Wen J, Takeshita A: Fluvastatin, a 3-hydroxy-3-methylglutaryl coenzyme A reductase inhibitor, attenuates left ventricular remodeling and failure after experimental myocardial infarction. *Circulation* 2002, 105:868-873
- Iwase M, Yokota M, Kitaichi K, Wang L, Takagi K, Nagasaka T, Izawa H, Hasegawa T: Cardiac functional and structural alterations induced

- by endotoxin in rats: importance of platelet-activating factor. *Crit Care Med* 2001, 29:609–617
13. Carmeliet P, Kieckens L, Schoonjans L, Ream B, van Nuffelen A, Prendergast G, Cole M, Bronson R, Collen D, Mulligan RC: Plasminogen activator inhibitor-1 gene-deficient mice. I. Generation by homologous recombination and characterization. *J Clin Invest* 1993, 92:2746–2755
  14. Kunishima S, Hayashi K, Kobayashi S, Naoe T, Ohno R: New enzyme-linked immunosorbent assay for glycoconjugates in plasma. *Clin Chem* 1991, 37:169–172
  15. Ishiguro K, Kojima T, Kadomatsu K, Nakayama Y, Takagi A, Suzuki M, Takeda N, Ito M, Yamamoto K, Matsushita T, Kusugami K, Muramatsu T, Saito H: Complete antithrombin deficiency in mice results in embryonic lethality. *J Clin Invest* 2000, 106:873–878
  16. Yamamoto K, Loskutoff DJ: Fibrin deposition in tissues from endotoxin-treated mice correlates with decreases in the expression of urokinase-type but not tissue-type plasminogen activator. *J Clin Invest* 1996, 97:2440–2451
  17. Yamamoto K, Takeshita K, Shimokawa T, Yi H, Isobe K, Loskutoff DJ, Saito H: Plasminogen activator inhibitor-1 is a major stress-regulated gene: implications for stress-induced thrombosis in aged individuals. *Proc Natl Acad Sci USA* 2002, 99:890–895
  18. Nishioka K, Kobayashi Y, Katayama I, Takijiri C: Mast cell numbers in diffuse scleroderma. *Arch Dermatol* 1987, 123:205–208
  19. Hara M, Ono K, Hwang MW, Iwasaki A, Okada M, Nakatani K, Sasayama S, Matsumori A: Evidence for a role of mast cells in the evolution to congestive heart failure. *J Exp Med* 2002, 195:375–381
  20. Kaikita K, Fogo AB, Ma L, Schoenhard JA, Brown NJ, Vaughan DE: Plasminogen activator inhibitor-1 deficiency prevents hypertension and vascular fibrosis in response to long-term nitric oxide synthase inhibition. *Circulation* 2001, 104:839–844
  21. Gersch C, Dewald O, Zoerlein M, Michael LH, Entman ML, Frangogiannis NG: Mast cells and macrophages in normal C57/BL/6 mice. *Histochem Cell Biol* 2002, 118:41–49
  22. Askari AT, Brennan M-L, Zhou X, Drinko J, Morehead A, Thomas JD, Topol EJ, Hazen SL, Penn MS: Myeloperoxidase and plasminogen activator inhibitor 1 play a central role in ventricular remodeling after myocardial infarction. *J Exp Med* 2003, 197:615–624
  23. Hattori N, Degen JL, Sisson TH, Liu H, Moore BB, Pandrangi RG, Simon RH, Drew AF: Bleomycin-induced pulmonary fibrosis in fibrinogen-null mice. *J Clin Invest* 2000, 106:1341–1350
  24. Brown NJ, Vaughan DE, Fogo AB: The renin-angiotensin-aldosterone system and fibrinolysis in progressive renal disease. *Semin Nephrol* 2002, 22:399–406
  25. Yamamoto K, Saito H: A pathological role of increased expression of plasminogen activator inhibitor-1 in human or animal disorders. *Int J Hematol* 1998, 68:371–385
  26. Zaman AK, Fujii S, Sawa H, Goto D, Ishimori N, Watano K, Kaneko T, Furumoto T, Sugawara T, Sakuma I, Kitabatake A, Sobel BE: Angiotensin-converting enzyme inhibition attenuates hypofibrinolysis and reduces cardiac perivascular fibrosis in genetically obese diabetic mice. *Circulation* 2001, 103:3123–3128
  27. Macfelda K, Weiss TW, Kaun C, Breuss JM, Kapeller B, Zorn G, Oberndorfer U, Voegelé-Kadletz M, Huber-Beckmann R, Ullrich R, Binder BR, Losert UM, Maurer G, Pacher R, Huber K, Wojta J: Plasminogen activator inhibitor 1 expression is regulated by the inflammatory mediators interleukin-1 $\alpha$ , tumor necrosis factor- $\alpha$ , transforming growth factor- $\beta$  and oncostatin M in human cardiac myocytes. *J Mol Cell Cardiol* 2002, 34:1681–1691
  28. Carroll SM, Nimmo LE, Knoepfler PS, White FC, Bloor CM: Gene expression in a swine model of right ventricular hypertrophy: intercellular adhesion molecule, vascular endothelial growth factor and plasminogen activators are upregulated during pressure overload. *J Mol Cell Cardiol* 1995, 27:1427–1441
  29. Takeshita K, Yamamoto K, Ito M, Kondo T, Matsushita T, Hirai M, Kojima T, Nabeshima Y, Loskutoff DJ, Saito H, Murohara T: Increased expression of plasminogen activator inhibitor-1 with fibrin deposition in a murine model of aging, “klotho” mouse. *Semin Thromb Hemost* 2002, 28:545–553
  30. Ono K, Matsumori A, Shioi T, Furukawa Y, Sasayama S: Cytokine gene expression after myocardial infarction in rat hearts: possible implication in left ventricular remodeling. *Circulation* 1998, 98:149–156
  31. Wiman B, Andersson T, Hallqvist J, Reuterwall C, Ahlbom A, deFaire U: Plasma levels of tissue plasminogen activator/plasminogen activator inhibitor-1 complex and von Willebrand factor are significant risk markers for recurrent myocardial infarction in the Stockholm Heart Epidemiology Program (SHEEP) study. *Arterioscler Thromb Vasc Biol* 2000, 20:2019–2023
  32. Vaughan DE, Rouleau JL, Ridker PM, Arnold JM, Menapace FJ, Pfeffer MA: Effects of ramipril on plasma fibrinolytic balance in patients with acute anterior myocardial infarction. *HEART Study Investigators. Circulation* 1997, 96:442–447
  33. Sinkovic A: Pretreatment plasminogen activator inhibitor-1 (PAI-1) levels and the outcome of thrombolysis with streptokinase in patients with acute myocardial infarction. *Am Heart J* 1998, 136:406–411
  34. Ruoss SJ, Hartmann T, Caughey GH: Mast cell tryptase is a mitogen for cultured fibroblasts. *J Clin Invest* 1991, 88:493–499
  35. Marone G, de-Crescenzo G, Adt M, Patella V, Arbustini E, Genovese A: Immunological characterization and functional importance of human heart mast cells. *Immunopharmacology* 1995, 31:1–18
  36. Laine P, Kaartinen M, Penttilä A, Panula P, Paaonen T, Kovanen PT: Association between myocardial infarction and the mast cells in the adventitia of the infarct-related coronary artery. *Circulation* 1999, 99:361–369
  37. Patella V, Marino I, Arbustini E, Lampater-Schummert B, Verga L, Adt M, Marone G: Stem cell factor in mast cells and increased mast cell density in idiopathic and ischemic cardiomyopathy. *Circulation* 1998, 97:971–978
  38. Matsumoto T, Wada A, Tsutamoto T, Ohnishi M, Isono T, Kinoshita M: Chymase inhibition prevents cardiac fibrosis and improves diastolic dysfunction in the progression of heart failure. *Circulation* 2003, 107:2555–2558
  39. Wojta J, Kaun C, Zorn G, Ghannadan M, Hauswirth AW, Sperr WR, Fritsch G, Printz D, Binder BR, Schatzl G, Zwirner J, Maurer G, Huber K, Valent P: C5a stimulates production of plasminogen activator inhibitor-1 in human mast cells and basophils. *Blood* 2002, 100:517–523
  40. Lyons RM, Gentry LE, Purchio AF, Moses HL: Mechanism of activation of latent recombinant transforming growth factor- $\beta$ 1 by plasmin. *J Cell Biol* 1990, 110:1361–1367
  41. Carmeliet P, Moons L, Lijnen R, Baes M, Lemaitre V, Tipping P, Drew A, Eeckhout Y, Shapiro S, Lupu F, Collen D: Urokinase-generated plasmin activates matrix metalloproteinases during aneurysm formation. *Nat Genet* 1997, 17:439–444
  42. Hopkins WE, Fujii S, Sobel BE: Synergistic induction of plasminogen activator inhibitor type-1 in HEP G2 cells by thrombin and transforming growth factor- $\beta$ . *Blood* 1992, 79:75–81
  43. Yamamoto K, Loskutoff DJ: Expression of transforming growth factor- $\beta$  and tumor necrosis factor- $\alpha$  in the plasma and tissues of mice with lupus nephritis. *Lab Invest* 2000, 80:1561–1570
  44. Reisdorf P, Lawrence DA, Sivan V, Klising E, Martin MT: Alteration of transforming growth factor-beta1 response involves down-regulation of Smad3 signaling in myofibroblasts from skin fibrosis. *Am J Pathol* 2001, 159:263–272
  45. Lindstedt KA, Wang Y, Shiota N, Saarinen J, Hyytiäinen M, Kokkonen JO, Keski-Oja J, Kovanen PT: Activation of paracrine TGF- $\beta$ 1 signaling upon stimulation and degradation of rat serosal mast cells: a novel function for chymase. *EMBO J* 2001, 15:1377–1388